Radiation Damage Effects and Operation of the LHCb Vertex Locator

K. Akiba, M. Alexander, W. Barter, L. Bell, G. Bogdanova, S. Borghi, T. Bowcock, E. Buchanan, J. Buytaert, S. de Capua, S. Chen, P. Collins, A. Crocombe, E. Dall'Occo, C. Dean, F. Dettori, K. Dreimanis, G. Dujany, L. Eklund, T. Evans, M. Gersabeck, T. Gershon, T. Hadavizadeh, J. Harrison, K. Hennessy, W. Hulsbergen, D. Hutchcroft, E. Jans, M. John, P. Kopciewicz, P. Koppenburg, G. Lafferty, T. Latham, A. Leflat, M. Majewski, F. Marinho, J. Mylroie-Smith, A. Oblakowska-Mucha, C. Parkes, A. Pearce, A. Poluektov, A. Pritchard, W. Qian, S. Redford, S. Richards, K. Rinnert, E. Rodrigues, P. Rodriguez, M. Schiller, M. Smith, T. Szumlak, M. van Beuzekom, J. Velthuis, V. Volkov, H. Wark, A. Webber, and M. Williams

***Abstract*— Vertex locator (VELO) is a silicon microstrip detector situated around the interaction point in the large Hadron Collider beauty (LHCb) spectrometer at the Large Hadron Collider. The LHCb experiment is dedicated to studying charge conjugation and parity symmetry violation in the heavy flavor sector and rare decays of B mesons. The precise reconstruction of both the primary and secondary vertices, obtained by the VELO, is crucial in the selection of signal events containing b and c quarks and lifetime measurements. VELO consists of two retractable parts that operate at 8 mm from the interaction region. Its proximity to proton beams makes the LHCb VELO a place for studying radiation damage effects in silicon detectors in proton–proton and heavy-ion collisions. The latest results from radiation damage studies and their impact on the operation of the LHCb VELO after the first data-taking period (Run I) and the ongoing Run II are presented in this paper. The main macroscopic parameters, influenced by particle fluence, are described along with selected methods of their monitoring. All the results show that VELO sustains the impact of high fluence of radiation, and its performance will not change significantly until the end of Run II.**

***Index Terms*— Depletion voltage, effective doping, leakage current, large Hadron Collider beauty (LHCb), radiation damage, silicon detector, vertex locator (VELO).**

Manuscript received March 8, 2018; accepted April 3, 2018. Date of publication April 10, 2018; date of current version May 16, 2018. This work was supported in part by the National Research Center, Poland under Grant UMO-2016 /21/B/ST2/01083 and in part by the Faculty of Physics and Applied Computer Science AGH UST statutory tasks under Grant 11.11.220.01/4 within subsidy of Ministry of Science and Higher Education.

K. Akiba and F. Marinho are with the Instituto de Fisica, Universidade Federal do Rio de Janeiro, Rio de Janeiro 21941-972, Brazil.

M. Alexander, C. Dean, L. Eklund, and M. Schiller are with the School of Physics and Astronomy, University of Glasgow, Glasgow G12 8QQ, U.K.

W. Barter, S. Borghi, S. de Capua, S. Chen, G. Dujany, M. Gersabeck, J. Harrison, G. Lafferty, C. Parkes, A. Pearce, E. Rodrigues, P. Rodriguez, M. Smith, A. Webber, and M. Williams are with the School of Physics and Astronomy, University of Manchester, Manchester M13 9PL, U.K.

L. Bell, E. Dall'Occo, W. Hulsbergen, E. Jans, P. Koppenburg, and M. van Beuzekom are with the Nikhef National Institute for Subatomic Physics, NL-1009 Amsterdam, The Netherlands.

G. Bogdanova, A. Leflat, and V. Volkov are with the Institute of Nuclear Physics, Moscow State University, Moscow 119991, Russia.

T. Bowcock, F. Dettori, K. Dreimanis, K. Hennessy, D. Hutchcroft, J. Mylroie-Smith, A. Pritchard, K. Rinnert, and H. Wark are with the Oliver Lodge Laboratory, University of Liverpool, Liverpool L69 7ZE, U.K.

E. Buchanan, S. Richards, and J. Velthuis are with the H.H. Wills Physics Laboratory, University of Bristol, Bristol BS8 1TL, U.K.

J. Buytaert and P. Collins are with the European Organization for Nuclear Research, CH-1211 Geneva, Switzerland.

A. Crocombe, T. Gershon, T. Latham, and A. Poluektov are with the Department of Physics, University of Warwick, Coventry CV4 7AL, U.K.

T. Evans, T. Hadavizadeh, M. John, W. Qian, and S. Redford are with the Department of Physics, University of Oxford, Oxford OX1 3RH, U.K.

P. Kopciewicz, M. Majewski, A. Oblakowska-Mucha, and T. Szumlak are with the Faculty of Physics and Applied Computer Science, 11AGH University of Science and Technology, PL-30-059 Krakow, Poland (e-mail: Agnieszka.Mucha@ agh.edu.pl).

Color versions of one or more of the figures in this paper are available online at http://ieeexplore.ieee.org.

Digital Object Identifier 10.1109/TNS.2018.2824618

I. Introduction

THE large Hadron Collider beauty (LHCb) detector is a single-arm forward spectrometer designed for studying heavy flavor physics at the Large Hadron Collider (LHC). The detector includes a high precision tracking system containing a silicon-strip detector surrounding the proton–proton interaction region [vertex locator (VELO)], one silicon-strip detector before the magnet (TT), and three tracking stations behind the magnet (T1–T3), as shown in Fig. 1. Each station comprises one silicon inner tracker and four layers of gas straw tubes (outer tracker). The tracking system provides a measurement of charged particle momentum with a relative uncertainty that varies from 0.5% to 1.0% at low momentum and 200 GeV, respectively. Two ring-imaging Cherenkov detectors provide efficient identification of charged particles with momenta up to 100 GeV. A complete description of the LHCb spectrometer can be found in [1].

Up until the end of 2017, 7.63 fb^{-1} of integrated luminosity, originating from proton–proton interactions at $\sqrt{s} = 7 - 13$ TeV, where s is the square of center-of-mass energy, has been delivered to the LHCb detector. In addition, the LHCb collected data samples of ultrarelativistic proton-lead collisions at $\sqrt{s_{\text{NN}}} = 5$ and 8.16 TeV and lead–lead collisions at $\sqrt{s} = 5$ TeV. The former sample corresponds to 32.3 nb^{-1}, whereas the latter corresponds to about 5.6 μb^{-1} of integrated luminosity.

II. Vertex Locator

The VELO is a silicon microstrip detector positioned around the interaction point (IP). VELO plays the main role in the

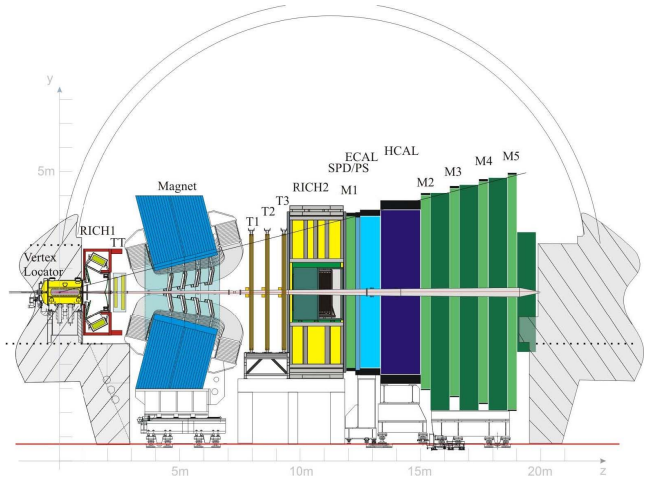

Fig. 1. Vertical cross section through the LHCb spectrometer. The proton–proton IP inside VELO is visible in the left part of the figure.

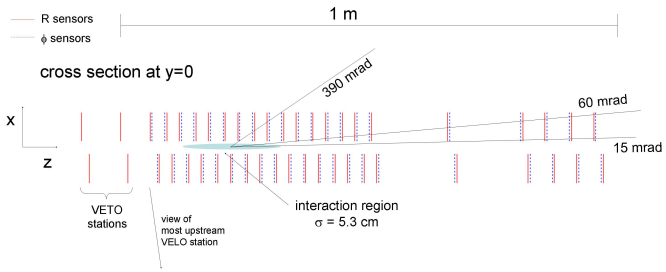

Fig. 2. Schematic of VELO sensors along the z-direction. Red solid and blue dotted line: R-type and Φ-type sensors, respectively. The measure of the horizontal size (σ) of the interaction region is shown.

primary and secondary vertex reconstructions, which is vital for discriminating heavy flavor hadrons in the high level trigger and the precise lifetime measurements [2].

The VELO consists of two movable halves that can be retracted up to 29 mm to avoid the risk of damage from the LHC beam during injection. Each half consists of 21 modules that operate at a secondary vacuum and are separated from the primary LHC vacuum by a 300-μm aluminum RF-foil (Fig. 2). A VELO module consists of two 300-μm-thick semicircular sensors with 2048 strips; they provide measurements of the radial coordinate (R-type sensor) and the azimuthal angle (Φ-type sensor). Sensor pitches vary within the range of 35 and 101 μm. Strips are routed via a double metal layer that carries the collected signal to the front-end electronics. All but two of the VELO sensors are oxygenated n^+-on-n (n-type implant in an n-type bulk with a back p-type implant); the remaining two are n^+-on-p. Four pile-up veto modules (which contain only an R sensor) are located upstream of the interaction region. An evaporative CO_2 cooling system keeps the sensors at temperatures below -5 °C to avoid reverse annealing. The nominal operation temperature, maintained by the main chiller, is -30 °C, and goes up to -6 °C when the front-end electronics of the sensors is switched ON during data taking, as shown in Fig. 3. The flexible and easy to operate cooling system enables the efficient

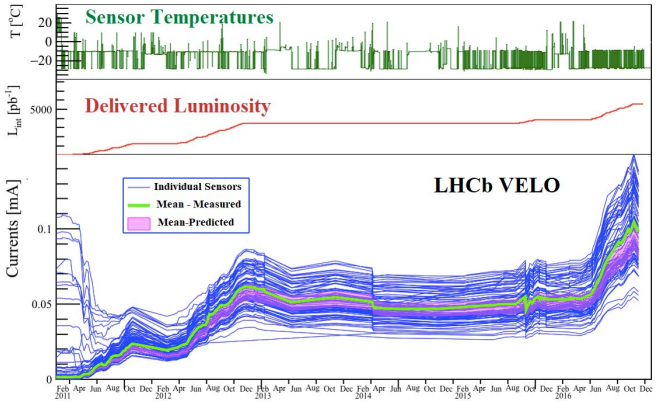

Fig. 3. Leakage current for the VELO sensors as function of time (bottom), delivered luminosity (middle), and sensor temperatures (top). The VELO sensors operate at -30 °C when the front-end electronics is OFF and at -8 °C during data taking. Some occasional warmings during assembly time are also present.

change of the temperature set point for dedicated scans or tests.

III. Radiation Environment

The innermost region of the active silicon is 8.2 mm from the LHC beam. The VELO sensors are subjected to extremely high fluence—up to 10.1×10^{13} 1 MeV n_{eq}/cm^2 per 1 fb^{-1}, as shown in Fig. 4. It means that till the end of 2017, the inner part of the sensors was irradiated to about 4.0×10^{14} 1 MeV n_{eq}/cm^2. The flux of particles is highly nonuniform with a strong dependence on both the radius and z position of a station. Because of the proximity of VELO to the IP, the main origin of the particle radiation is the prompt production of hadrons (pions, protons, and neutrons) in proton or ion collisions.

The impact of the incident particles on the silicon lattice properties pertains to the creation of deep-level defects, whose concentration can greatly exceed the shallow dopants. Thus, after irradiation, the electrical properties of silicon change significantly [4]. New energy levels created in the silicon bandgap play the roles of either generation or recombination centers in the depletion region. Charge carriers created by a traversing particle may also be trapped in the trapping centers created by defects, causing a delay in the signals collected by the electrodes. In general, the degrading influence of the particle radiation manifests itself in three important ways: 1) increasing leakage current; 2) changing the effective doping concentration in silicon (which has an impact on the operation voltage needed for total depletion); and 3) losing charge collection efficiency (CEE) [3].

The radiation-induced effects accumulate over time and cause progressive degradation in the detector. Hence, regular monitoring of radiation damage to the VELO sensors is essential to ensure the proper running conditions of the detector. In addition, the bias voltage needs to be adjusted to guarantee excellent performance in the whole data-taking period. Since the VELO sensors cannot be taken out of the LHCb spectrometer, three methods of monitoring are regularly performed: 1) current–voltage (IV) scans; 2) current–temperature (IT) scans; and 3) CCE scans.

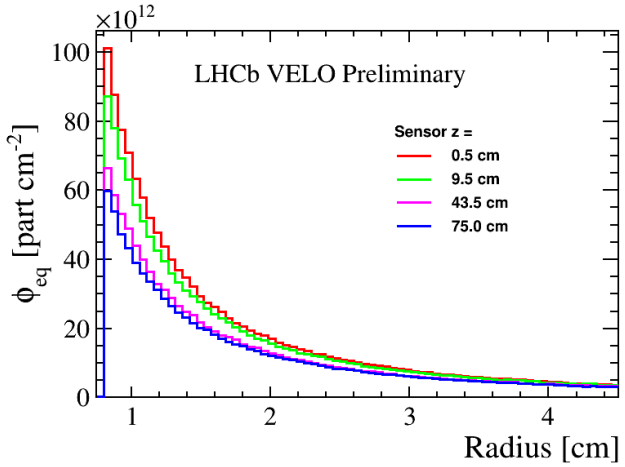

Fig. 4. Predicted radial dependence of fluence in selected VELO sensors. Inset: sensors' position along the beam line. Plots correspond to the integrated luminosity of 1 fb^{-1}, fluence is simulated for protons colliding at center of mass energy $\sqrt{s} = 13$ TeV.

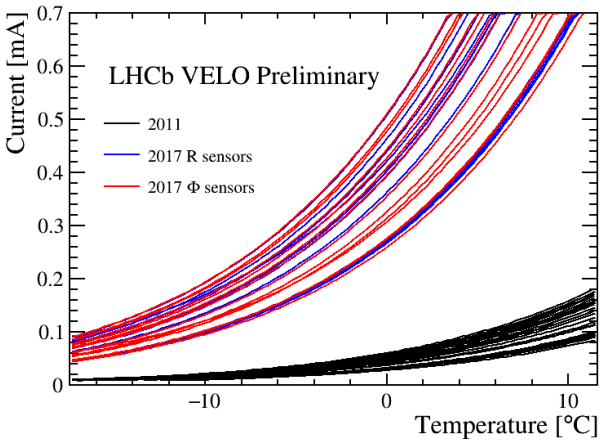

Fig. 5. Leakage currents measured across the selected VELO sensors plotted as a function of their temperature. The results were obtained using IT scans taken in 2011 and 2017, and correspond to the delivered luminosities of 0.8 and 6.5 fb^{-1}, respectively. The lines represent results of the procedure where the model described in (1) was fit to data points collected during respective IT scans.

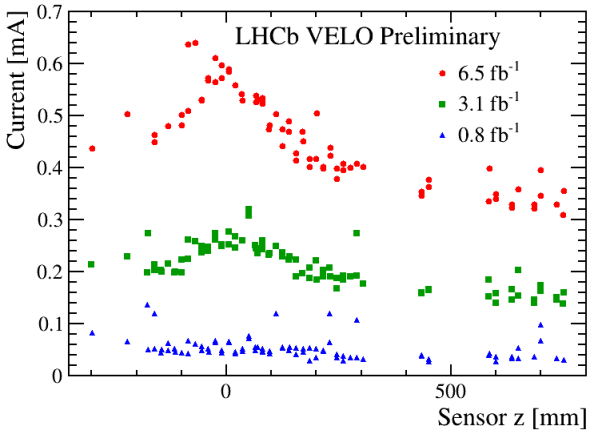

Fig. 6. Mean leakage currents measured across the VELO sensors plotted as a function of their position along the beam line (z-axis in the LHCb coordinate system). The currents are scaled to 0 °C. Two sets of points (blue triangles and green squares) represent data taken during Run I and correspond to the delivered luminosities of 0.8 and 3.1 fb^{-1}, respectively. The third one (red circles) represents data taken in Run II and corresponds to the delivered luminosity of 6.5 fb^{-1}.

IV. Measurement of the Sensor Currents

Leakage current in an irradiated silicon sensor is caused mainly by electron–hole generation centers lying close to the midgap, where an electron is excited to the conduction band through the intermediate level created by the defects. Since the concentration of defects rises with the fluence, the leakage current also increases. The sensor leakage current may be also caused by charge deposits on the surface or defects in the bulk of the detector. The former can arise in the production stage (from scratches, nonuniformities in the cut edges, etc.) and disappear after the sensor is exposed to high particle fluence [3].

The increase of leakage current in the bulk of the sensor rises linearly with the equivalent fluence. This dependence for the VELO sensors is shown in Fig. 4. The change in the leakage currents of all VELO sensors are found to evolve proportionally to the delivered luminosity, whereas it is relatively flat during the long breaks between data-taking periods. A typical increase is about 1.9 μA per 0.1 fb^{-1} of the delivered luminosity.

Since the bulk generation current is mainly the result of thermal excitation, it varies exponentially with temperature

$$I(T) \propto T^2 \exp\left(\frac{E_{geff}}{2k_B T}\right) \tag{1}$$

where T stands for the absolute temperature, $E_{geff} = 1.21$ eV is the silicon effective energy gap, and k_B is Boltzmann's constant. This feature is exploited during the measurements of the current as a function of the sensor temperature (IT scans). Such tests may be done only during LHC shutdowns without collisions. From the exponential behavior of the IT scans (see Fig. 5), the silicon effective gap can be determined. The first study showed a value of $E_{geff} = 1.16 \pm 0.06$ eV [3], which is statistically in agreement with the literature value of 1.21 eV [5]. It is worth noting that effective energy gap value decreases after irradiation [6]. The study on whether this tendency is also observed in the VELO sensors is ongoing.

A steady increase in measured leakage currents for the VELO sensors is expected as a result of accumulated particle fluence. The mean leakage current measured for three selected integrated luminosities of 0.8, 3.1, and 6.5 fb^{-1}, respectively, scaled to 0 °C as shown in Fig. 6. Apart from the increase in value, one can also note a significant variation of the currents depending on a sensor location along the beam. This is a consequence of the fact that the fluences seen by the sensors close to the luminous region are much higher than for the ones located further downstream. The difference in measured currents can be as high as 50%. The increase in value and spread between measured currents can also be seen in Fig. 5.

Sensor currents are also studied as a function of voltage. Current–voltage (IV) scans are taken with an automated procedure on a weekly basis, during periods between fills. The main aim is to monitor whether the sensor is fully depleted

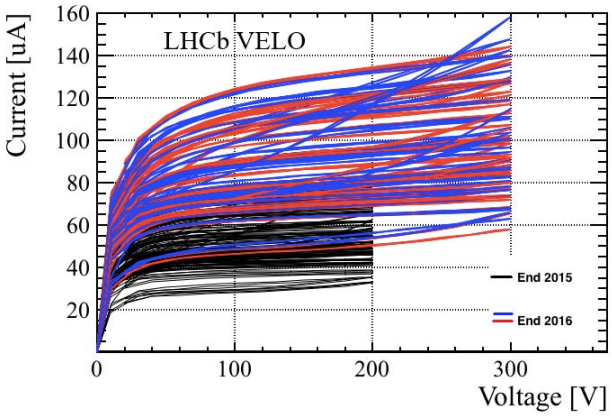

Fig. 7. IV scans of selected VELO sensors taken during Run II. Black lines: currents as a function of applied voltage for both types of sensors at the end of the year 2015 and delivered luminosity of 3.56 fb^{-1}. Blue and red lines: correspond to the R-type and Φ-type sensors, respectively, measured at the end of the year 2016 (5.7 fb^{-1}).

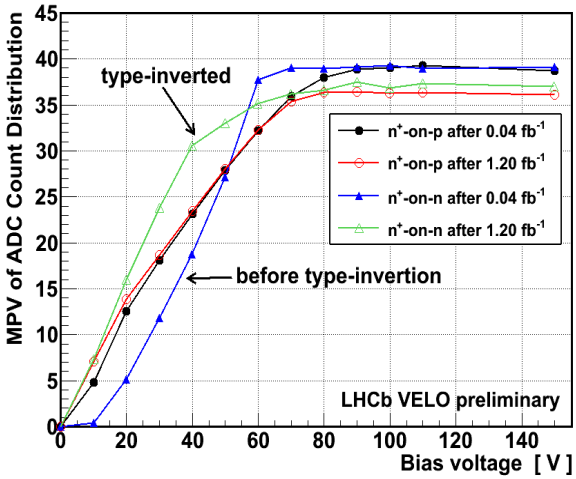

Fig. 8. MPV curves for n-on-n-type and n-on-p-type sensors as a function of bias voltage, before and after irradiation. In case of n-bulk sensor, for a given MPV, the depletion voltage decreases after type-inversion. This effect is not observed in p-bulk sensors, which are not type-inverted [3].

(the reverse-bias current saturates at high-bias voltages) and to look for a sudden rise preceding the breakdown. An example of IV scans taken during the Run II data-taking is presented in Fig. 7. The increase in currents due to radiation damage in the sensor bulk is clearly visible.

V. Effective Depletion Voltage

The bias voltage that is necessary to fully deplete each sensor is proportional to the effective doping concentration N_{eff} (the difference between the donor and acceptor concentration)

$$V = \frac{e}{2\varepsilon}|N_{\text{eff}}|d^2 \tag{2}$$

where d is the sensor thickness, e is the elementary charge, and ε is the permittivity constant.

After irradiation, the silicon dopant (phosphorus) may be captured by defects, losing its original function as donor or acceptor. In n-type sensors, the formation of vacancy-phosphorus defects causes the removal of donors, a lack of negative carriers, and a decrease in the positive space charge. In addition, the ionized defects may emit electrons to the conduction band, become positive acceptors, and form an additional negative space charge [7]. Operationally, a change in the space charge works like a change in a doping concentration; thus, it influences the carrier transport in the depleted layer. So, the bias voltage must be raised proportionally to the increase of the space charge to ensure that the charge deposited by the traversing particle is fully collected.

The depletion voltage of the VELO sensors was determined before the assembly of the whole detector by measuring the dependence of the sensor capacitance on the voltage. At present, a different method has been implemented. A dedicated scan, whose aim is to verify whether the applied voltage is sufficient for full depletion and to determine the cluster finding efficiency (CFE), is performed. During the data-taking periods (5–6 times a year), special data are taken and CCE scans are carried out [3]. A sensor under test has its bias voltage scanned from zero to the maximum predicted value and is excluded from the track fit procedure. A particle track is extrapolated to the test sensor using hits in the adjacent sensors which play the role of a telescope. The deposited charge is measured in the strips of the test sensor at the interpolated region. The most probable value (MPV) of the ADC charge distribution is determined and plotted as a function of the increasing reverse voltage. When it reaches the plateau, it means that the sensor has become fully depleted. Thus, the effective depletion voltage (EDV) is established as the bias voltage that corresponds to 80% of the maximum MPV obtained during a voltage scan. Having done such a scan regularly, one can monitor which sensor is fully depleted and adjust the voltage as necessary. An example of one of the Run I CCE scans is shown in Fig. 8.

In n-type sensors, the original space charge in the depleted region is positive; however, after irradiation, the contribution of acceptor like defects is eventually higher than the positive space charge created by the donors. As a result, the electrical behavior of an n-type sensor changes toward a p-type and the EDV declines. This phenomenon (called *type-inversion*) was expected in the VELO sensors and occurred in the n^+-on-n sensors at the fluence of the order of 10^{13} 1 MeV n_{eq}/cm^2 [8]. After the type-inversion, the detector acts as a p-type; N_{eff} and the EDV rise linearly with the fluence. This behavior is clearly visible in Fig. 9; in the case of the n^+-on-n sensors, the EDV originally decreases and then, after type-inversion, goes up. The EDV of the two n^+-on-p sensors rises proportionally to the fluence, without type-inversion, as predicted [3]. It is visible that this increase started at lower fluences than in n^+-on-n sensors and the rise is faster.

If a sensor is not fully depleted, the CCE is reduced; thus, the reverse bias of a sensor must be increased to compensate for this effect. Before installation, a depletion voltage below 70 V was sufficient for full depletion; during Run I, the sensors were biased up to 150 V, whereas 250 V was applied in 2016 to the most irradiated sensors close to the IP. In 2017, the bias voltage was set to 300 V for all sensors.

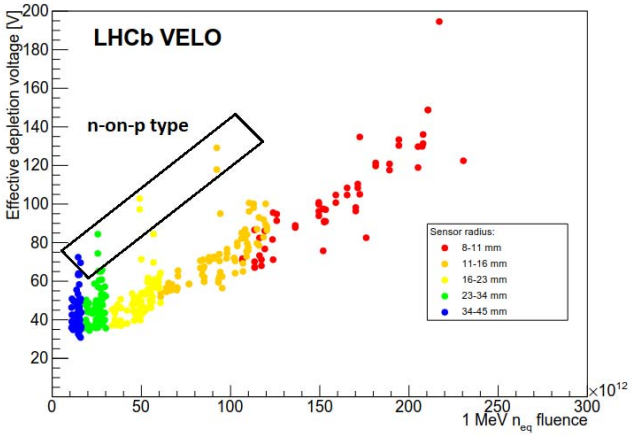

Fig. 9. Change in EDV of the VELO sensors with fluence. Different colors correspond to sensor radius mentioned in the inset. The two n^+-on-p sensors (indicated in rectangle) have the highest EDV value. Data were taken during the Run II data-taking period, in the year 2017 and correspond to approximately 5.6 fb^{-1} of luminosity.

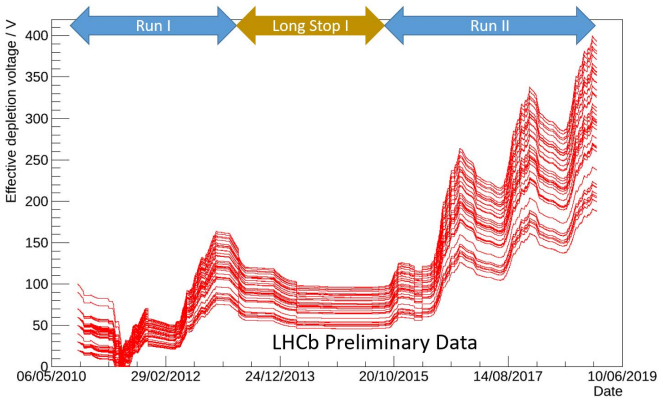

Fig. 10. Hamburg model prediction of change in EDV of VELO. Lines correspond to different sensors.

The gradual increase in the bias voltage according to the obtained values from the CCE scans is necessary to avoid operation in overdepletion region which may cause the smaller charge sharing and reduce the detector resolution.

The need to increase the voltage necessary for full depletion of the whole sensor has become a challenge for VELO in the ongoing Run II data-taking period. The LHCb delivered luminosity may exceed 9 fb^{-1} by the end of 2018. This means that the fluence accumulated by the inner part of the sensors would be above 5×10^{14} 1 MeV n_{eq}/cm^2 by that time.

The change of the bias voltage was done according to the CCE scans and prediction of the evolution of EDV based on the Hamburg model [8]. It assumes that the effective doping concentration varies with annealing time, temperature, and the equivalent fluence. The parametrization of both the beneficial and reverse annealing has been adjusted to the VELO operational temperature. The fluence was calculated based on simulation and the LHCb luminosity measurement. In Fig. 10, the prediction of the EDV increase up to the year 2018 is presented. The VELO was designed to withstand 8 fb^{-1} of integrated luminosity at the center-of-mass

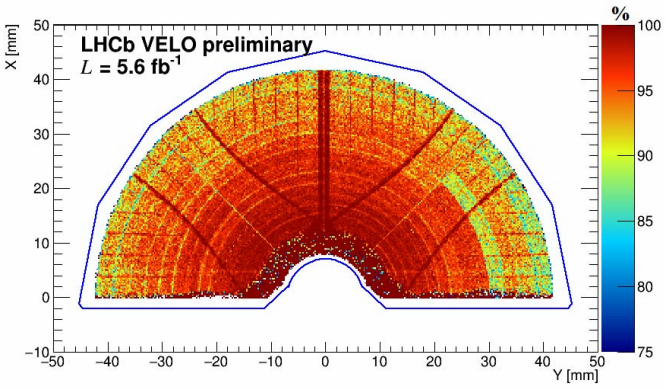

Fig. 11. CFE map of one of the downstream VELO R-type sensors. Position of straight dark red lines agrees with RLs, and radial colored regions represent the decrease of CFE.

energy $\sqrt{s} = 14$ TeV [1]. The Hamburg model prediction and simulation of fluence expected for the actual LHC parameters show that the operational bias voltage will have to be increased to 450 V, which is still below the hardware limit.

VI. Cluster Finding Efficiency

The CCE scans described in Section V can also be used to monitor the efficiency of finding and reconstructing the charge clusters. A cluster is understood as the one or several neighboring strips with charge above a particular threshold. The CFE is defined as a fraction of the tracks that left charge clusters in the test sensors in the position that is predicted by the interception of the hits from adjacent sensors [3]. These measurements are performed during the data-taking period, with full operational condition, i.e., nominal bias voltage. While analyzing the CCE scans, one can search for charge clusters in the selected strips; therefore, these data can also be used to study the CFE in different regions of the sensor.

Before irradiation, the CCE was greater than 99%; but soon afterward, it turned out that it dropped to as far as 94%. It was surprising that the largest changes occurred in the outer regions of those sensors that are most distant from the collision point (and the only R-types). This degradation was observed over the whole data-taking period; it finally dropped to 90% in the outer sensor regions. A map of the CFE taken after the Run I data period was over is shown in Fig. 11.

The detailed study showed that the decrease of the CCE was caused by the so-called *second metal layer effect* [3]. In the VELO sensors, the signal induced in a strip by a passing particle is transferred to the amplifier by a routing line (RL). In the case of R-type sensors, the RLs are perpendicular to the strips (see Fig. 12). The strips in the outer sensor region are more than three times wider than in the inner part, while the RLs width remains constant. Also, the strip pitch in the outer region is twice as big as in the inner one. So, the released charge is shared between the adjacent strip and the RL. When the distance to the RL is shorter than to the strip, more charge is induced in the RL (causing a loss of signal charge in the strip). The CFE as a function of distance to the RL for different places of the released charges is presented in Fig. 13.

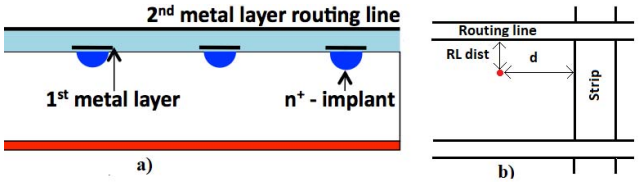

Fig. 12. (a) Layout of second metal layer in R-type VELO sensor [3]. (b) Location of RL and strip. Red dot: position of traversing particle. d is the distance to the nearest strip, whereas RL dist—to RL.

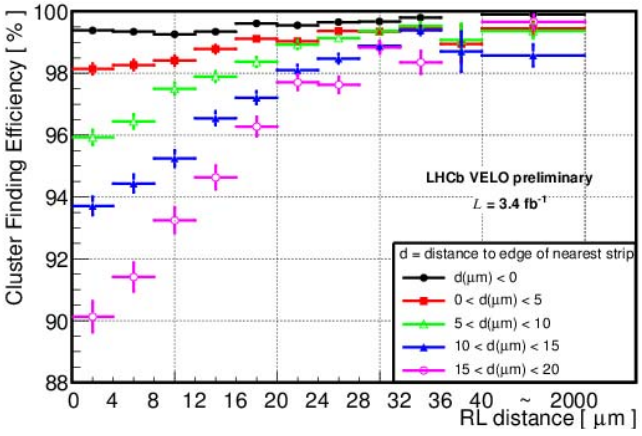

Fig. 13. CFE as a function of distance to RL. Different colors mark increasing distances to the nearest strip.

The most serious drop occurs when the distance to the RL is much smaller than the distance to the closest strip. In the Φ-type sensors, where RLs are over the strips, a loss of CFE was not observed. Instead, it was noticed that in R-type sensors, the amount of charge collected is lower than in Φ-type sensors, and the cluster size is bigger. It has been observed that the decrease of CCE is stronger when the sensors were more severely irradiated [2]. The explanation of the connection between the *second metal layer effect* and irradiation is not straightforward and is being investigated.

The lower CFE can potentially have an adverse impact on the overall tracking efficiency and pose a serious problem for physics analyses that rely on acceptance corrections, such as the absolute cross section measurements. Appropriate corrections have been, therefore, introduced in both tracking and simulation software. The signal-to-noise ratio is monitored, and the results and predictions show that until the end of the current data-taking period (Run II), it will be well above of a value of 10, which is conventionally regarded as the minimum for the operation of a silicon detector [2].

VII. Radiation Damage Due to Ion Runs

In 2015, the LHCb experiment collected data during LHC ion runs. For the VELO detector, the biggest concern was that the multiplicity of events in lead collisions would be much higher than during proton–proton ones. In fact, in the very central collision, up to 35×10^3 particles may be produced; however, in the VELO acceptance, this number is twice as small. Simulations show that the accumulated dose obtained during the ion's runs would be equivalent to about 25 nb^{-1} of proton–proton interaction; thus, it does not cause significant additional radiation damage [9]. Due to the large density of the particles, the currents in the VELO sensor could at the most increase by 4 μA.

VIII. Summary

Precise vertex reconstruction, tracking, and fast response are the main features of the VELO silicon micro-strip detector. The silicon sensitivity to radiation is a main challenge for operation in dense environment of particles at LHC. Thus, the impact of fluence on the VELO silicon sensors is monitored during whole data-taking period using dedicated scans. All changes (such as increase of leakage currents, change in the EDV, and decrease of the CFE) are examined. Appropriate precautions are taken to mitigate the damaging effects (i.e., cooling of the sensors) and maximize the performance. The detailed study of the implications of the *second metal layer effects*, which impacts the track reconstruction efficiency, is ongoing. All radiation damage effects are within expectations, and the prediction shows that VELO will perform without major degradation until the end of Run II period, collecting data that are equivalent to 10 fb^{-1} of integrated luminosity.

References

[1] A. A. Alves *et al.*, "The LHCb detector at the LHC," *J. Instrum.*, vol. 3, p. S08005, Aug. 2008, doi: 0.1088/1748-0221/3/08/S08005.
[2] R. Aaij *et al.*, "Performance of the LHCb vertex locator," *J. Instrum.*, vol. 9, p. P09007, Sep. 2014, doi: 10.1088/1748-0221/9/.09/P09007.
[3] A. Affolder, "Radiation damage in the LHCb vertex locator," *J. Instrum.*, vol. 8, p. P08002, Aug. 2013, doi: 10.1088/1748-0221/8/08/.P08002.
[4] I. Pintilie, G. Lindstroem, A. Junkes, and E. Fretwurst, "Radiation-induced point-and cluster-related defects with strong impact on damage properties of silicon detectors," *Nucl. Instrum. Methods Phys. Res. A, Accel. Spectrom. Detect. Assoc. Equip.*, vol. 611, no. 1, pp. 52–68, 2009, doi: 10.1016/j.nima.2009.09.065.
[5] A. Chilingarov, "Generation current temperature scaling," CERN, Genève, Switzerland, Tech. Rep. PH-EP-Tech-Note-2013-001, 2013.
[6] S. Wonsak, A. Affolder, G. Casse, P. Dervan, I. Tsurin, and M. Wormald, "Measurements of the reverse current of highly irradiated silicon sensors," *Nucl. Instrum. Methods Phys. Res. A, Accel. Spectrom. Detect. Assoc. Equip.*, vol. 796, pp. 126–130, Oct. 2015, doi: 10.1016/j.nima.2015.04.027.
[7] M. Moll, "Radiation damage in silicon particle detectors," Ph.D. dissertation, Dept. Phys., Hamburg Univ., Hamburg, Germany, 1999.
[8] A. Affolder *et al.*, "Silicon detectors for the sLHC," *Nucl. Instrum. Methods Phys. Res. A, Accel. Spectrom. Detect. Assoc. Equip.*, vol. 658, no. 1, pp. 11–16, 2011, doi: 10.1016/j.nima.2011.04.045.
[9] B. Schmidt, "Results from pPb collisions and prospects for heavy-ion interactions with LHCb," *Nucl. Particle Phys. Proc.*, vols. 276–278, pp. 84–89, Jul. 2016, doi: 10.1016/j.nuclphysbps.2016.05.016.